

1 Timing of the Arabia-Eurasia continental collision -
2 Evidence from detrital zircon U-Pb geochronology of the
3 Red Bed Series strata of the NW Zagros hinterland,
4 Kurdistan region of Iraq

5

6 **Renas I. Koshnaw^{1*}, Daniel F. Stockli², and Fritz Schlunegger¹**

7 *¹Institute of Geological Sciences, University of Bern, Baltzerstrasse 1+3, CH-3012 Bern,*
8 *Switzerland*

9 *²Department of Geological Sciences, Jackson School of Geosciences, University of Texas*
10 *at Austin, Austin, TX 78712, USA*

11

12 * Corresponding author

13

14

15

16

17

18

19

20

21

22 **ABSTRACT**

23 One of the major debated aspects of the Zagros orogenic system is the timing of
24 onset of continental collision between Arabia and Eurasia. The Zagros hinterland in the
25 Kurdistan region of Iraq contains a ca. 2 km-thick clastic depositional sequence of the
26 Red Bed Series (RBS) that rests unconformably on the Arabian foreland and structurally
27 below the Main Zagros Fault, which carries the allochthonous volcanoclastic rocks of the
28 Walash-Naopurdan groups. Detrital zircon (DZ) U-Pb geochronology constrains both the
29 depositional age and the provenance of the RBS and pinpoint the timing of initial arrival
30 of Eurasian sediment on the Arabian plate. The youngest DZ U-Pb ages for the laterally-
31 extensive (ca. 150 km) basal RBS (Suwais unit) imply a middle Oligocene (ca. 26 Ma)
32 maximum depositional age. The provenance data reveal dominant DZ U-Pb age modes of
33 late Paleocene (~55-60 Ma) and middle Eocene (~37-44 Ma) and, importantly, presence
34 of ca. 10-15% DZ grains that are unequivocally derived from Eurasia, incl. Jurassic (150-
35 200 Ma) and late Paleozoic (270-380 Ma) DZ age modes. These data suggest that the
36 RBS deposits were mainly sourced from forearc/arc-related terranes along the SW
37 margin and hinterland of Eurasia. We advocate that by ca. 26 Ma Neotethys oceanic crust
38 had been consumed and that Arabia-Eurasia continental collision well was underway as
39 indicated by deposition of strata with Eurasian provenance on the Arabian margin. These
40 DZ U-Pb data from the RBS highlight the significance of provenance data from
41 synorogenic deposits in revealing the timing of initial continent collision by document the
42 earliest arrival of upper-plate sediment on the lower plate.

43

44 **Keywords:** Zagros, continental collision, U-Pb geochronology, detrital zircon,
45 provenance, Red Bed Series

46 **INTRODUCTION**

47 The Zagros collisional zone is one of the most prominent and recent collisional segments
48 of the Alpine-Himalayan orogenic system and formed in response to the northward
49 subduction of the Neo-Tethys oceanic crust beneath the Eurasian continental plate,
50 culminating in the continent-continent collision between the Arabian and Eurasian plates
51 (e.g., Alavi, 1994; Hessami, 2001). The initiation of Arabia-Eurasia continent-continent
52 collision remains highly debated, due to the complex along-strike nature, poor
53 preservation the early synorogenic structural and depositional orogenic record, and the
54 complicated tectonic phases that included Late Cretaceous ophiolite obduction and island
55 and/or volcanic arc collisions prior to the continent-continent collision. Whereas studies
56 had suggested a possible pre-Cenozoic onset of continental collision, it is now well
57 understood that Late Cretaceous to early Cenozoic ophiolite obduction and arc accretion,
58 recorded in the proto-Zagros foreland basins, were not related to the continental collision
59 and not yet involve Eurasia (Homke et al., 2009; Saura et al., 2011). Timing constraints
60 for the Cenozoic Zagros continent-continent collision vary considerably and range
61 between Eocene to Miocene (e.g., Horton et al., 2008; Fakhari et al., 2008; Homke et al.,
62 2009; Gavillot et al., 2010; Agard et al., 2011; Ballato et al., 2011, McQuarrie and van
63 Hinsbergen, 2013; Zhang et al., 2016; Pirouz et al., 2017; Barber et al., in press).
64 Constraining the inception of the Arabian and Eurasian plates collision is vital for the
65 understanding of initial continental collision as well as the broader tectonic and
66 geodynamic evolution of the Middle East, including the relationship between rifting in

67 the Gulf of Aden/Red Sea system and collision in the Zagros-Bitlis system. This study
68 focuses on the earliest synorogenic deposits of the Red Bed Series (RBS), that rests
69 unconformably on the Arabian foreland and structurally below a low-angle thrust - the
70 Main Zagros Fault (MZF) –that carries the allochthonous volcanoclastic rocks of the
71 Walash-Naopurdan groups and the Sanandaj-Sirjan Zone (SSZ) in its hanging wall (Al-
72 Barzinjy, 2005; Jassim and Goff, 2006; Hassan et al., 2014). Over ca. 150 km along-
73 strike, the RBS is irregularly truncated by the MZF, providing a synorogenic sedimentary
74 record during allochthonous thrust sheet emplacement (Figs. 1 and 2). In this paper, we
75 present new DZ U-Pb age data to elucidate the timing of deposition and characterize the
76 provenance of the RBS and discuss the implications for the timing of the continental
77 collision between Arabia and Eurasia.

78

79 **THE RED BED SERIES STRATA**

80 The Red Bed Series (RBS) is a Cenozoic siliciclastic sequence deposited in a laterally
81 extensive (ca. 150 km) depositional system in the interior of the NW Zagros fold-thrust
82 belt, on the Arabian side of the suture zone in the footwall of the MZF (Fig. 2). These
83 deposits rest unconformably on deformed Cretaceous rocks of the Arabian platform
84 (Karim et al., 2011; Hassan et al., 2015). Along strike, the RBS basin deposits define
85 several NW-SE oriented discrete depocenters with a composite total preserved
86 stratigraphic thickness of ca. 2 km (Al-Barzinjy, 2005). In the study area, NW of the
87 Dukan Lake, the RBS has a thickness of ca. 1400 m (Fig. 3) and consists of alternating
88 mudstone and sandstone as well as conglomerates and limestone beds with calcareous
89 sandstone. These deposits can be subdivided into three major units: Suwais, Govanda,

90 and Merga units, which were deposited in estuarine, fluvial, and alluvial environments
91 (Jassim and Goff, 2006; Alsultan and Gayara, 2016; Abdula et al., 2018).

92

93 **METHODS AND SAMPLING**

94 Detrital zircon (DZ) U-Pb geochronology has been shown to be a powerful tool for
95 identifying the provenance of sedimentary basins and constraining the timing of
96 maximum depositional ages (MDA) in volcanically active convergent belts (Fedó et al.,
97 2003; Dickinson and Gehrels, 2009). In this study, we present 679 new DZ U-Pb ages
98 from six Red Bed Series samples (Fig. 3): three from Suwais unit (CH17S10, SH17S4,
99 MT17S5) and three from Merga unit (CH17M6, CH17M5, CH17M4). Four samples are
100 from the same section (CH-) and two Suwais unit samples are from along-strike localities
101 (SH-, MT-) (Fig. 1). All ages were obtained using the Laser Ablation Inductively
102 Coupled Plasma Mass Spectrometry (LA-ICP-MS) following procedures outlined in Hart
103 et al. (2016) at the University of Texas at Austin UTChron Geo- and Thermochronometry
104 laboratories. See GSA Data Repository¹ item for detailed analytical procedures and all
105 analytical data.

106

107 **RESULTS**

108 All Red Bed Series samples show major DZ age components that cluster in the late
109 Paleocene and the middle Eocene. The three Suwais unit samples (SH17S4, CH17S10,
110 MT17S5) display two major age peaks at 56-58 (late Paleocene) and 37-45 Ma (middle
111 Eocene). Samples from the Merga unit (CH17M6, CH17M5, CH17M4), which are
112 stratigraphically younger, show correlative DZ age signatures of 37-44 Ma (middle

113 Eocene) and 55-60 Ma (late Paleocene), except for sample CH17M4 that show only a
114 major middle Eocene peak (Fig. 4; GSA Data Repository¹). In addition to these two
115 dominant DZ U-Pb age components, the RBS samples exhibit notable subsidiary Late
116 Cretaceous (65-120 Ma), Jurassic (150-200 Ma), late Paleozoic (270-380 Ma), and
117 Precambrian (500-700 Ma) DZ age components. The three youngest zircon grains from
118 the basal Suwais unit yielded a mean age of 26.0 ± 0.9 Ma ($n=3$, MSDW=4.7) and from
119 the stratigraphically higher Merga a mean age of 34.8 ± 0.6 Ma ($n=3$, MSDW=1.6).

120

121 **DISCUSSION**

122 **Detrital zircon provenance**

123 The late Paleocene and middle Eocene dominant DZ U-Pb age components encountered
124 in the Red Bed Series (RBS) samples suggest a provenance from (i) the Walsh-
125 Naopurdan Groups that are thrust on top of the RBS, (ii) the magmatic portions of the
126 SSZ, and (iii) the Urumieh-Dokhtar magmatic zone (UDMZ), which are all associated
127 with the Eurasian plate (Figs. 1 and 4). The Walsh-Naopurdan Groups of the Zagros
128 Suture Zone are likely the equivalent of the Gaveh-Rud Domain forearc deposits in the
129 Iranian Zagros farther to the SE in the Lorestan salient (Sadeghi and Yassaghi, 2016).
130 Reported ages for volcanoclastic forearc/arc-related sequences are middle Eocene (Agard
131 et al., 2005; Homke et al., 2009; Aswad et al., 2014) and late Eocene (Ali et al., 2013).
132 As for the upper-plate hinterland, the metamorphosed SSZ contains several igneous
133 intrusions, incl. the Piranshahr and Kamyaran massifs that span the time interval between
134 the late Paleocene-early Eocene and the middle Eocene ages (Mazhari et al., 2009; Azizi
135 et al., 2011). Farther to the NE, the Andean-type UDMZ continental arc is dominated by

136 voluminous intrusive and extrusive rocks with a peak magmatism age of 55-37 Ma
137 (Verdel et al., 2011; Chiu et al., 2013).

138 Among the minor DZ U-Pb age components of the RBS, the Jurassic (150-200
139 Ma) and the late Paleozoic (270-380 Ma) are unequivocally indicative of sources from
140 the SSZ and the broader Eurasian hinterland and have not been reported from the Arabian
141 plate. The 150-200 Ma DZ ages are sourced from numerous plutons in the SSZ (Chiu et
142 al., 2013), while the 270-380 Ma age component is linked to Hercynian magmatic
143 sources (Stampfli et al., 2013). Based on these provenance data, the RBS detritus,
144 unconformably deposited on Arabia, was derived from the convergent southwestern
145 margin and orogenic hinterland of Eurasia.

146

147 **Timing of deposition**

148 The age of the youngest DZ grains from samples from the bottom of the Suwais unit
149 within the lower part of the RBS strata, suggest that the RBS deposition started sometime
150 during the middle Oligocene. Each of the three Suwais samples, geographically 10s of
151 kilometers apart along strike, contained a single young grain that combined yielded a
152 mean age of ca. 26 Ma, implying a middle Oligocene depositional age for the Suwais
153 unit. This MDA is significantly younger than published Paleocene-Eocene ages for the
154 Suwais unit based on the planktonic foraminifera (Al-Barzinjy, 2005 and Hassan, 2012).
155 These conflicting biostratigraphic and isotopic ages likely point to reworking of the
156 Paleocene-Eocene microfossils – a hypothesis supported by a dominant Paleocene-
157 Eocene DZ age peak. The sparse, but consistent youngest middle Oligocene DZ U-Pb
158 ages support a laterally synchronous onset of lower Suwais deposition over ca. 150 km

159 along strike. Regionally, the basal Suwais unit unconformably overlies folded Triassic-
160 Cretaceous Qulqula Formation or Cretaceous Bekhma and Shiranish Formations. While
161 Karim and others (2011) and Hassan and others (2014) proposed an apparent
162 conformable contact between the RBS and the Maastrichtian Tanjero Formation, the ~26
163 Ma MDA for the Suwais unit implies a hiatus of ~40 m.y. and a disconformable contact
164 between the RBS and the Tanjero Formation.

165

166 **Timing of the Arabia-Eurasia continental collision**

167 The Red Bed Series in NE Iraqi Kurdistan is characterized by an unequivocally Eurasian
168 DZ U-Pb provenance signature, a middle Oligocene maximum depositional age of ~26
169 Ma, and widespread regional unconformity with a 40 m.y. hiatus prior to RBS deposition.
170 These observations provide clear evidence for the minimum age for the Arabia-Eurasia
171 continental collision during the middle Oligocene. These new timing constraints support
172 an earlier timing for the onset of continent-continent collision by the middle Oligocene.
173 These findings are in general agreement with estimates on basis of plate circuit
174 reconstructions and foreland basin sedimentation patterns (e.g., Saura et al., 2015;
175 McQuarrie and van Hinsbergen, 2013; Pirouz et al., 2017; Zadeh et al., 2017). They,
176 however, do not preclude an Eocene inception of collisional deformation (e.g., Ballato et
177 al. 2011, Mouthereau et al., 2012; Barber et al, in press).

178

179 **CONCLUSIONS**

180 Our new DZ U-Pb age data along with the structural and stratigraphic setting of the RBS
181 deposits, in the present-day interior of the Zagros fold-thrust belt, indicate the minimum

182 age for the Arabia-Eurasia continent-continent collision in the middle Oligocene at ca. 26
183 Ma. The basal RBS, which is structurally truncated by the MZF low-angle thrust and
184 buried by allochthonous thrust sheets, was unconformably deposited on the Arabian
185 plate. The basal RBS deposits of the Suwais unit yielded a middle Oligocene (ca. 26 Ma)
186 maximum depositional age and exhibits provenance data indicative of derivation from
187 forearc and arc-related terranes and the hinterland along the southwestern margin of the
188 Eurasia. These data argue for an onset of continent-continent collision and arrival of the
189 Eurasia-sourced sediment on the Arabian plate by at least the middle Oligocene.

190

191 **FIGURE CAPTIONS**

192 Figure 1. Left: Regional tectonic map of the Middle East showing the Main Zagros Fault
193 (MZF) that separates Arabia and Eurasia, as well as the Arabian plate motion velocities
194 and directions, which are relative to Eurasia (Koshnaw et al., 2017 and references
195 therein). The black rectangle represents the outline of the geologic map to the right.
196 Right: Simplified geologic map of the study area (Koshnaw et al., 2017 and references
197 therein) depicting the location of the rock samples that used in this study. The blue
198 dashed line represents the international border.

199

200 Figure 2. Schematic cross-section illustrating the structural and stratigraphic settings of
201 the Red Bed Series deposits in the NW Zagros fold-thrust belt, and the apparent locations
202 of the sample. MDA: maximum depositional age.

203

204

205 Figure 3. Generalized composite stratigraphic column of the Red Bed Series illustrating
206 the key lithostratigraphic units and the apparent location of the dated rock samples in the
207 NW of the study area. Stratigraphic data are from Jassim and Goff (2006), Alsultan and
208 Gayara (2016), Abdula et al., (2018) and fieldwork from this study.

209

210 Figure 4. Top: Detrital zircon U-Pb age distribution plots of samples from the Suwais and
211 Merga units that show significant probability density peaks (histograms bin size is 20
212 Ma; Vermeesch, 2012) during Paleogene. Bottom: Percentages of the potential source
213 components from the Suwais unit samples.

214

215 ¹GSA Data Repository item 201Xxxx, U-Pb data of the newly analyzed zircon grains are
216 available online at www.geosociety.org/pubs/ft20XX.htm, or on request from
217 editing@geosociety.org or Documents Secretary, GSA, P.O. Box 9140, Boulder, CO
218 80301, USA.

219

220 **ACKNOWLEDGMENTS**

221 This research was partially funded by the State Secretariat for Education, Research and
222 Innovation of Switzerland via the Swiss Government Excellence Scholarship that
223 awarded to Renas I. Koshnaw. We thank Idrees Nadir and Nihad Karo at Salahaddin
224 University-Erbil as well as staff and students at the University of Texas at Austin
225 UTChron Geo- and ThermoChronometry laboratories for their assistance.

226

227 **REFERENCES CITED**

- 228 Abdula, R. A., Chicho, J., Surdashy, A., Nourmohammadi, M. S., Hamad, E.,
229 Muhammad, M. M., ... & Ashoor, A., 2018, Sedimentology Of The Govanda
230 Formation At Gali Baza Locality, Kurdistan Region, Iraq. *Iraqi Bulletin of Geology
231 and Mining*, 14(1), 1-12.
- 232 Agard, P., Omrani, J., Jolivet, L. and Mouthereau, F., 2005, Convergence history across
233 Zagros (Iran): constraints from collisional and earlier deformation. *International
234 journal of earth sciences*, 94(3), pp. 401-419.
- 235 Agard, P., Omrani, J., Jolivet, L., Whitechurch, H., Vrielynck, B., Spakman, W., Wortel,
236 R., 2011, Zagros orogeny: a subduction-dominated process. *Geological
237 Magazine*, 148(5-6), 692-725.
- 238 Al-Barzinjy, S.T., 2005, Stratigraphy and basin analysis of the Red Series from NE Iraq,
239 Kurdistan region, unpublished PhD dissertation, University of Sulaimaniya, Iraq
- 240 Alavi, M., 1994, Tectonics of the Zagros orogenic belt of Iran: new data and
241 interpretations. *Tectonophysics*, 229(3-4), 211-238.
- 242 Ali, S. A., Buckman, S., Aswad, K. J., Jones, B. G., Ismail, S. A. & Nutman, A. P., 2013,
243 The tectonic evolution of a Neo-Tethyan (Eocene-Oligocene) island-arc (Walash
244 and Naopurdan groups) in the Kurdistan region of the Northeast Iraqi Zagros Suture
245 Zone. *Island Arc*, 22 (1), 104-125.
- 246 Alsultan, H. A. A. and A. D. Gayara, 2016, Basin Development of the Red Bed Series,
247 NE Iraq. *Journal of University of Babylon*, 24(2), 435-447.
- 248 Aswad, K. J., Al-Samman, A. H., Aziz, N. R., & Koyi, A. M., 2014, The geochronology
249 and petrogenesis of Walash volcanic rocks, Mawat nappes: constraints on the
250 evolution of the northwestern Zagros suture zone, Kurdistan Region, Iraq. *Arabian
251 Journal of Geosciences*, 7(4), 1403-1432.
- 252 Azizi, H., Tanaka, T., Asahara, Y., Chung, S. L., & Zarrinkoub, M. H., 2011,
253 Discrimination of the age and tectonic setting for magmatic rocks along the Zagros
254 thrust zone, northwest Iran, using the zircon U–Pb age and Sr–Nd isotopes. *Journal
255 of Geodynamics*, 52(3-4), 304-320.
- 256 Ballato, P., Uba, C.E., Landgraf, A., Strecker, M.R., Sudo, M., Stockli, D.F., Friedrich,
257 A. and Tabatabaei, S.H., 2011, Arabia-Eurasia continental collision: Insights from
258 late Tertiary foreland-basin evolution in the Alborz Mountains, northern
259 Iran. *Bulletin*, 123(1-2), pp.106-131.
- 260 Barber, D. E., D. F. Stockli, B. K. Horton, R. I. Koshnaw, in press, Cenozoic Exhumation
261 and Foreland Basin Evolution of the Zagros Orogen during Arabia-Eurasia
262 Collision, Western Iran. *Tectonics*
- 263 Chiu, H.Y., Chung, S.L., Zarrinkoub, M.H., Mohammadi, S.S., Khatib, M.M. and Iizuka,
264 Y., 2013, Zircon U–Pb age constraints from Iran on the magmatic evolution related
265 to Neotethyan subduction and Zagros orogeny. *Lithos*, 162, pp.70-87.
- 266 Dickinson, W.R. and Gehrels, G.E., 2009, Use of U–Pb ages of detrital zircons to infer
267 maximum depositional ages of strata: a test against a Colorado Plateau Mesozoic
268 database. *Earth and Planetary Science Letters*, 288(1-2), pp.115-125.
- 269 Fakhari, M.D., Axen, G.J., Horton, B.K., Hassanzadeh, J. and Amini, A., 2008, Revised
270 age of proximal deposits in the Zagros foreland basin and implications for Cenozoic
271 evolution of the High Zagros. *Tectonophysics*, 451(1-4), pp.170-185.
- 272 Fedo, C.M., Sircombe, K.N. and Rainbird, R.H., 2003, Detrital zircon analysis of the
273 sedimentary record. *Reviews in Mineralogy and Geochemistry*, 53(1), pp.277-303.

- 274 Gavillot, Y., Axen, G.J., Stockli, D.F., Horton, B.K. and Fakhari, M.D., 2010, Timing of
275 thrust activity in the High Zagros fold-thrust belt, Iran, from (U-Th)/He
276 thermochronometry. *Tectonics*, 29(4).
- 277 Hart, N. R., Stockli, D. F., & Hayman, N. W. (2016). Provenance evolution during
278 progressive rifting and hyperextension using bedrock and detrital zircon U-Pb
279 geochronology, Mauléon Basin, western Pyrenees. *Geosphere*, 12(4), 1166-1186.
- 280 Hassan, M. M., Sedimentology of the Red Beds in NE Iraq, 2012, Ph.D. thesis, School of
281 Earth and Environmental Sciences, University of Wollongong.
282 <http://ro.uow.edu.au/theses/3831>
- 283 Hassan, M., Jones, B.G., Buckman, S., Al-Jubory, A.I. and Al Gahtani, F.M., 2014,
284 Provenance of Paleocene–Eocene red beds from NE Iraq: constraints from
285 framework petrography. *Geological Magazine*, 151(06), pp. 1034-1050.
- 286 Hassan, M.M., Jones, B.G., Buckman, S., Al Jubory, A.I., and Ismail, S.A., 2015, Source
287 area and tectonic provenance of Paleocene–Eocene red bed clastics from the
288 Kurdistan area NE Iraq: Bulk-rock geochemistry constraints: *Journal of African*
289 *Earth Sciences*, v. 109, p. 68-86.
- 290 Hessami, K., Koyi, H.A., Talbot, C.J., Tabasi, H. and Shabanian, E., 2001, Progressive
291 unconformities within an evolving foreland fold–thrust belt, Zagros
292 Mountains. *Journal of the Geological Society*, 158(6), pp.969-981.
- 293 Homke, S., Vergés, J., Serra-Kiel, J., Bernaola, G., Sharp, I., Garcés, M., Montero-Verdú,
294 I., Karpuz, R. and Goodarzi, M.H., 2009, Late Cretaceous–Paleocene formation of
295 the proto–Zagros foreland basin, Lurestan Province, SW Iran. *Geological Society of*
296 *America Bulletin*, 121(7-8), pp.963-978.
- 297 Horton, B.K., Hassanzadeh, J., Stockli, D.F., Axen, G.J., Gillis, R.J., Guest, B., Amini,
298 A., Fakhari, M.D., Zamanzadeh, S.M. and Grove, M., 2008, Detrital zircon
299 provenance of Neoproterozoic to Cenozoic deposits in Iran: Implications for
300 chronostratigraphy and collisional tectonics. *Tectonophysics*, 451(1-4), pp.97-122.
- 301 Jassim, S.Z. and Goff, J.C., 2006, *Geology of Iraq*. Dolin, Prague and Moravian
302 Museum. Brno, 2006.–341 pp.
- 303 Karim, K.H., Koyi, H., Baziany, M.M. and Hessami, K., 2011, Significance of angular
304 unconformities between Cretaceous and Tertiary strata in the northwestern segment
305 of the Zagros fold–thrust belt, Kurdistan Region, NE Iraq. *Geological*
306 *Magazine*, 148(5-6), pp.925-939.
- 307 Koshnaw, R. I., Horton, B. K., Stockli, D. F., Barber, D. E., Tamar-Agha, M. Y., &
308 Kendall, J. J., 2017, Neogene shortening and exhumation of the Zagros fold-thrust
309 belt and foreland basin in the Kurdistan region of northern Iraq. *Tectonophysics*,
310 694, 332-355.
- 311 Mazhari, S.A., Bea, F., Amini, S., Ghalamghash, J., Molina, J.F., Montero, P., Scarrow,
312 J.H. and Williams, I.S., 2009, The Eocene bimodal Piranshahr massif of the
313 Sanandaj–Sirjan Zone, NW Iran: a marker of the end of the collision in the Zagros
314 orogen. *Journal of the Geological Society*, 166(1), pp.53-69.
- 315 McQuarrie, N. and van Hinsbergen, D.J., 2013. Retrodeforming the Arabia-Eurasia
316 collision zone: Age of collision versus magnitude of continental
317 subduction. *Geology*, 41(3), pp.315-318.
- 318 Pirouz, M., Avouac, J.P., Hassanzadeh, J., Kirschvink, J.L. and Bahroudi, A., 2017, Early
319 Neogene foreland of the Zagros, implications for the initial closure of the Neo-

- 320 Tethys and kinematics of crustal shortening. *Earth and Planetary Science*
321 *Letters*, 477, pp.168-182.
- 322 Sadeghi, S. and Yassaghi, A., 2016, Spatial evolution of Zagros collision zone in
323 Kurdistan, NW Iran: constraints on Arabia–Eurasia oblique convergence. *Solid*
324 *Earth*, 7(2), 659-659.Saura, E., Garcia-Castellanos, D., Casciello, E., Parravano, V.,
325 Urruela, A. and Vergés, J., 2015, Modeling the flexural evolution of the Amiran and
326 Mesopotamian foreland basins of NW Zagros (Iran-Iraq). *Tectonics*, 34(3), pp.377-
327 395.
- 328 Saura, E., Vergés, J., Homke, S., Blanc, E., Serra-Kiel, J., Bernaola, G., & Sharp, I. R.,
329 2011, Basin architecture and growth folding of the NW Zagros early foreland basin
330 during the Late Cretaceous and early Tertiary. *Journal of the Geological*
331 *Society*, 168(1), 235-250.
- 332 Stampfli, G.M., Hochard, C., Vérard, C. and Wilhem, C., 2013, The formation of
333 Pangea. *Tectonophysics*, 593, pp.1-19.
- 334 Verdel, C., Wernicke, B.P., Hassanzadeh, J. and Guest, B., 2011, A Paleogene
335 extensional arc flare-up in Iran. *Tectonics*, 30(3).
- 336 Vermeesch, P., 2012, On the visualisation of detrital age distributions. *Chemical*
337 *Geology*, v.312-313, 190-194, doi: 10.1016/j.chemgeo.2012.04.021 0
- 338 Zadeh, P.G., Adabi, M.H., Hisada, K.I., Hosseini-Barzi, M., Sadeghi, A. and Ghassemi,
339 M.R., 2017, Revised version of the Cenozoic Collision along the Zagros Orogen,
340 Insights from Cr-spinel and Sandstone Modal Analyses. *Scientific reports*, 7(1),
341 p.10828.
- 342 Zhang, Z., Xiao, W., Majidifard, M.R., Zhu, R., Wan, B., Ao, S., Chen, L., Rezaeian, M.
343 and Esmaeili, R., 2017, Detrital zircon provenance analysis in the Zagros Orogen,
344 SW Iran: implications for the amalgamation history of the Neo-
345 Tethys. *International Journal of Earth Sciences*, 106(4), pp.1223-1238.
346

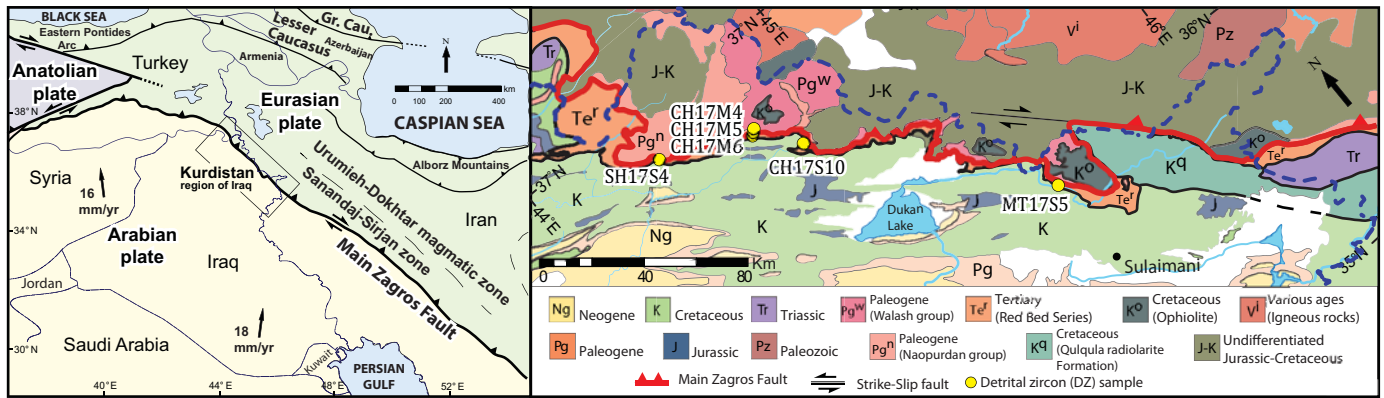


Figure 1

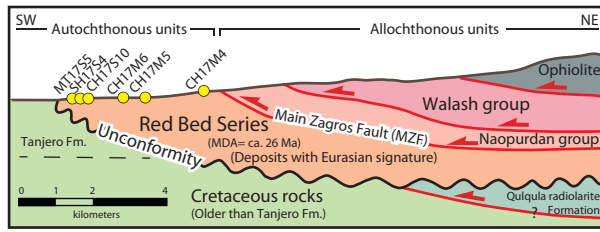


Figure 2

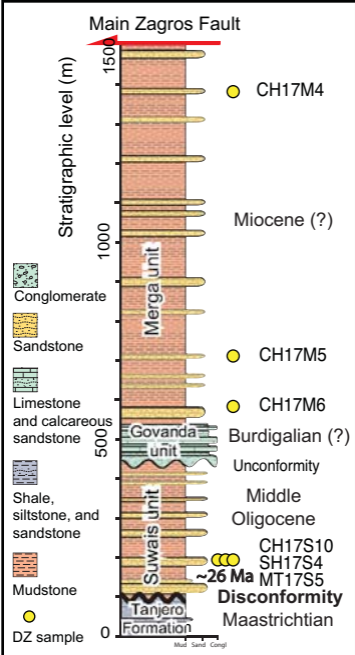


Figure 3

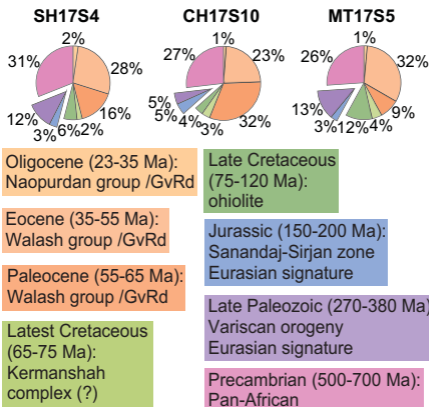
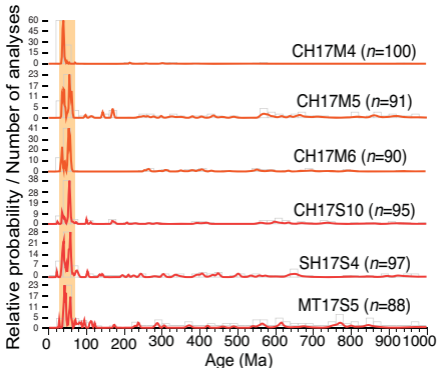


Figure 4